ELSEVIER

Journal of Marine Systems 38 (2002) 109–123

JOURNAL OF MARINE SYSTEMS

www.elsevier.com/locate/jmarsys

Grazing of phytoplankton by microzooplankton in the Barents Sea during early summer

Peter G. Verity[a,*], P. Wassmann[b], M.E. Frischer[a], M.H. Howard-Jones[a], A.E. Allen[a]

[a] *Skidaway Institute of Oceanography, 10 Ocean Science Circle, Savannah, GA 31411, USA*
[b] *Norwegian College of Fishery Science, University of Tromso, N-9000 Tromso, Norway*

Received 12 July 2001; accepted 1 February 2002

Abstract

Phytoplankton growth rates and grazing losses to microzooplankton were determined in surface waters of the central Barents Sea during a cruise in June/July 1999. Five stations were occupied which had been studied repeatedly over the past 15–20 years. Dilution experiments using chlorophyll *a* (chl *a*) as a tracer were used to estimate daily rates in three size fractions; image-analyzed fluorescence microscopy provided quantitative estimates of standing stocks of auto- and heterotrophic nano- and microplankton. Phytoplankton contributed the largest share of protistan biomass, followed by bacteria and microzooplankton. On average, nanophytoplankton (<20 μm) contributed half of the microphytoplankton (<200 μm) biomass. All stocks were low relative to peak spring bloom concentrations reported in previous years. Different taxonomic groups of microzooplankton were relatively more important under the ice, in the marginal ice zone (MIZ), and in open water. Phytoplankton growth and microzooplankton grazing rates were 0.1 to 0.5 day^{-1}, and were closely coupled. Neither growth nor grazing rates alone was closely related to phytoplankton biomass, but the net difference between growth and grazing explained about 2/3 of the variance in chl *a* standing stocks. Grazing losses ranged from 64% to 97% of daily chl *a* production, and were greater for smaller size fractions. Growth and grazing coefficients of all size classes exhibited Q_{10}'s of 2–3. These results support the growing body of evidence that small-celled phytoplankton and zooplankton are ubiquitous and important in cold waters as well as temperate and tropical ecosystems.

Keywords: Arctic; Primary production; Grazing; Zooplankton; Barents Sea; Q_{10}; Size class

1. Introduction

The central Barents Sea is a productive Arctic ecosystem composed of numerous water masses including the northward-flowing Norwegian Coastal Current; the Norwegian Atlantic Current flowing easterly into the Barents Sea; and cold Arctic waters flowing south, meeting the warm Atlantic waters at the Polar Front (Loeng et al., 1997). This mixing of relatively nutrient-rich source waters supports a rich biota of higher trophic levels including capelin, cod, seabirds, and marine mammals (Sakshaug and Skjoldal, 1989; Sakshaug, 1991). The classical model for cold water ecosystems in general was developed from early studies in these waters, which focused on large phytoplankton as the food source for large copepods

* Corresponding author. Fax: +1-912-598-2310.
E-mail address: peter@skio.peachnet.edu (P.G. Verity).

0924-7963/02/$ - see front matter © 2002 Elsevier Science B.V. All rights reserved.
PII: S0924-7963(02)00172-0

and krill, which in turn were forage for marine mammals, fish, and birds (Gran, 1902).

With the re-discovery (Pomeroy, 1974; Azam et al., 1983) of the microbial food web first described a century ago (Lohmann, 1908), the traditional large cell/organism-based, short food chain paradigm of planktonic ecosystems has gradually been replaced by data showing that it is in fact the small cells and organisms which are the continuous workhorses of the euphotic zone. Diatoms are the seasonal workhorses, which come and go with silicate availability. These data have been accumulated primarily in temperate, subtropical, and tropical ecosystems for logistic and population density-derived reasons. But as our knowledge extends into polar waters, it is becoming apparent that micro-, nano-, and even picoplankton are much more important than previously thought in such cold waters (Verity and Vernet, 1992; Stoecker et al., 1995; Hansen et al., 1996; Nielsen and Hansen, 1999; Verity et al., 1999; Levinsen et al., 2000).

The goal of this study was to investigate the hypothesis that primary production by micro- and nanophytoplankton was significant during late spring/early summer in the central Barents Sea, and to determine the extent to which grazing by microzooplankton was a significant loss process in the water column. Previous studies have suggested this might be the case (Hansen et al., 1996), but there are also reports of mass sedimentation by the spring bloom in these waters (Wassmann et al., 1990), implying poor coupling to the zooplankton community. While the notion that plankton community structure to a large degree influences its function is becoming accepted (Verity and Smetacek, 1996; Wassmann, 2001), the exact mechanisms remain unclear. The present study addresses these issues in the central Barents Sea during early summer of 1999.

2. Materials and methods

2.1. Study region

Cruise ALV-3 sampled a series of nineteen stations at regular intervals across the central Barents Sea along the transect line shown in Fig. 1A; this transect has been sampled repeatedly for more than 20 years (e.g. Rey and Loeng, 1985; Skjoldal et al., 1987; Wassmann and Slagstad, 1993; Hansen and Jensen, 2000; citations therein). A diverse suite of other microbial parameters were collected as part of this study and are described elsewhere (Howard-Jones et al., 2002, this issue; Allen et al., 2002, this issue). The ship entered the marginal ice zone (MIZ) on July 1 and proceeded NNE until ice cover and thickness prevented further progress. This became the first 24-h experimental station; further information is given in Wassmann (2002, this issue). Four additional 24-h stations were conducted with ca. one day between the end of one station and the beginning of the next. Although they were conducted chronologically from north to south, they are listed here as south to north in order to correspond to the sequence order of transect stations (also south to north).

2.2. Phytoplankton growth and microzooplankton grazing

A dilution approach (Landry and Hassett, 1982; Landry, 1993) was used to determine the rates of herbivory by the microzooplankton community. Surface (0–1 m) water samples were collected at each of the five 24-h stations where floating sediment trap arrays were deployed (see Olli et al., 2002, this issue), either using acid-cleaned plastic bucket or 10-l Niskin bottles. Water was apportioned into two carboys for use as dilution water and experimental water. All equipment that came in contact with seawater (e.g. carboys, tubing, filtration equipment, and meshes) were stored in dilute acid between uses and rinsed with deionized water immediately prior to use. Dilution water was prepared by gravity filtration directly from carboys through sequential 3.0 and 0.2 μm Gelman capsule filters into 25 l polyethylene carboys. This process removed all phytoplankton including the smallest picoplankton and most bacteria, which has been shown previously (Verity et al., 1996) and was confirmed here by pigment fluorometry and microscopy. The capsule filters were soaked in 10% HCl for 1 day before initial use and in-between uses. Prior to each use, ca. 10 l of seawater were passed through them to remove any traces of acid. Post-cruise nutrient analyses showed that the concentrations of ammonium, nitrate + nitrite, silicate, and phosphate were the same in seawater before and after capsule filtration, as previously shown in more oligotrophic waters (Verity et al., 1996) and also reported in Norwegian coastal

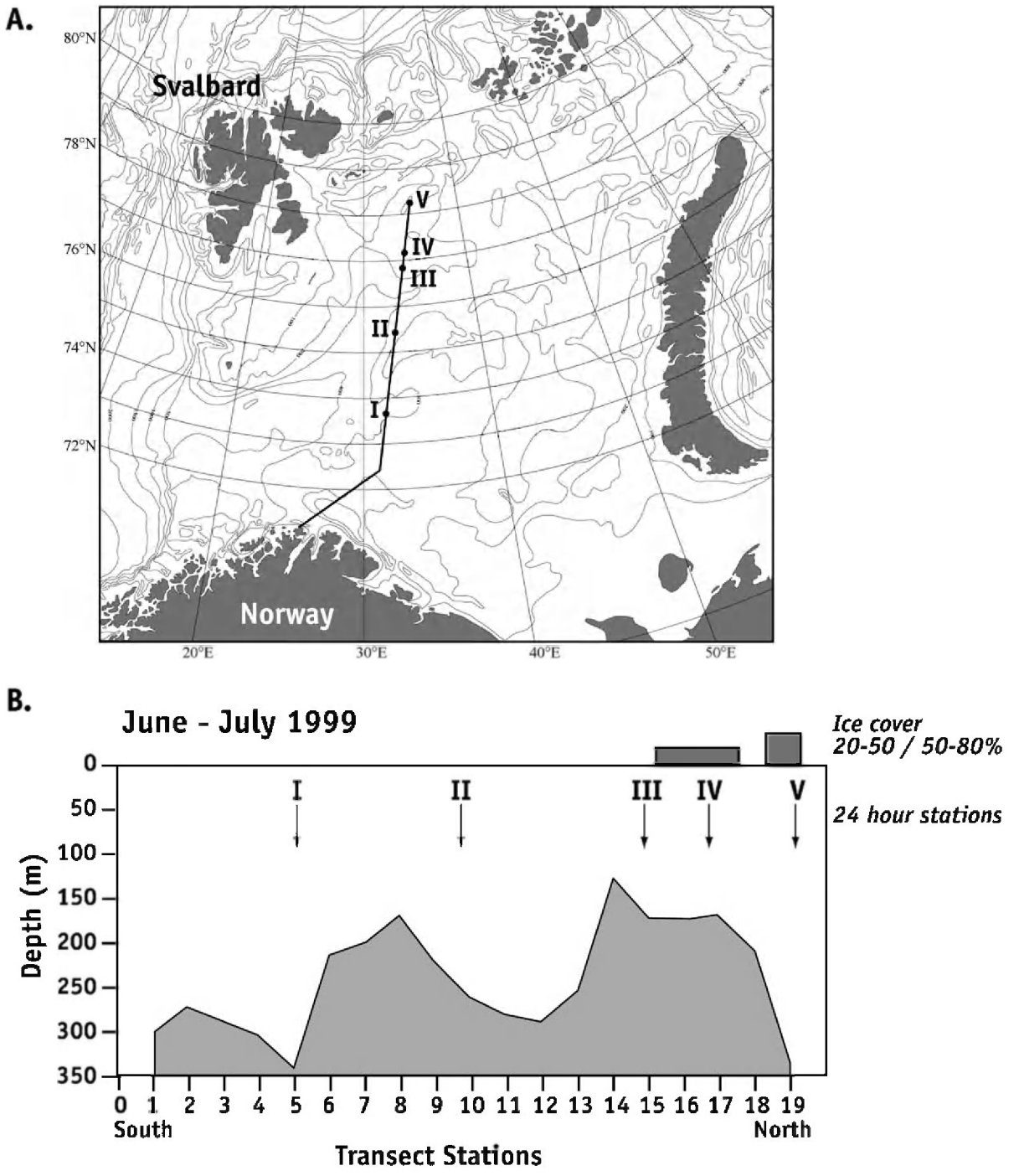

Fig. 1. (A) Map showing the cruise track of the R/V Jan Mayen and locations of the five experimental stations in July 1999. (B) The locations of the five stations with respect to bottom topography and surface ice cover.

waters (Archer et al., 2000). Cartridges were changed after the third experiment.

Concurrently, experimental water was gently sieved through 200 μm Nitex mesh into a separate acid-cleaned polyethylene carboy. Two-liter Teflon bottles served as incubation vessels. Experimental water was gently added to dilution water to create five duplicated dilution treatments in 20% increments. Low concentrations of macronutrients (NO_3:NH_4:$Si(OH)_4$:PO_4 = 5:5:5:0.5 μM) were added during the experiments to minimize potential nutrient limitation. Bottles were incubated in flowing seawater in deck incubators covered with one layer of neutral density screening to match near-surface irradiance. Incubations began at various times during 1100–1700 h local time; the variation in start time was considered relatively unimportant given the ambient 24:0 L:D photoperiod. At T_0 and T_{24} hours, samples were collected to measure chlorophyll *a* (chl *a*) from all dilutions. Subsamples were passed through separate (non-sequential) 20 μm nylon and 8 μm polycarbonate meshes to create <20 and <8 μm size fractions. These were filtered in duplicate onto Gelman GF/F filters, stored at −20 °C in the dark, and measured fluorometrically after dark extraction into cold 90% acetone using a Turner-Designs fluorometer (Strickland and Parsons, 1972). Calibration factors were determined and checked at regular intervals using pigments derived from phytoplankton cultures and measured using HPLC. The range in coefficients of variation for chl *a* was typically 3% to 5% (see Results). Nutrient samples were frozen at −20 °C and concentrations determined in the laboratory with an autoanalyzer (Føyn et al., 1981; Wassmann et al., 1990).

Phytoplankton growth rates and grazing by microzooplankton were estimated as described by Landry and Hassett (1982) and Landry (1993). Deviations from linearity in the relationship between apparent growth rate and dilution (Gifford, 1988; Gallegos, 1989) were not apparent in these experiments, similar to observations in Norwegian fjords (Verity and Vernet 1992; Archer et al., 2000).

2.3. Abundance and biomass of auto- and heterotrophic protists

Numerically abundant cells <200 μm, including ciliates, aplastidic flagellates and dinoflagellates (the microzooplankton), phytoplankton, and bacteria were enumerated in initial experimental samples. Subsamples were preserved in glutaraldehyde (final concentration = 0.3%) and then stained with 3–6-diaminoacridine hemisulfate (proflavin) for 1 min (5 μg ml^{-1} final concentration) and 4′ 6-diamindino-2-phenylindole (DAPI) for 4 min (5 μg ml^{-1} final concentration). Samples for bacteria were stained only with DAPI. Separate volumes were then filtered onto 0.2 and 0.8 μm black Nuclepore filters: bacteria were measured on the smaller pore-size filters, and phytoplankton and microzooplankton on the larger filters. To achieve an even distribution for counting and measurement purposes, black filters were placed on top of pre-wetted Whatman GF/F backing filters. After filtration, the damp filter was placed on a slide, covered with a drop of low fluorescence immersion oil and a cover slip, and frozen at −20 °C. Samples were analyzed upon return to the laboratory.

An Olympus BX-60 microscope equipped with 100 W Hg illumination was employed for cell measurements, with appropriate exciter/barrier filter sets for UV (335–365 nm), blue (435–490 nm), and green (510–560 nm) excitation. Dinoflagellates were distinguished from other flagellates based upon cell morphology and structure of the nucleus, especially the unique condensed chromosomes visible by DAPI staining. Heterotrophic and autotrophic cells were discriminated by the absence and presence of autofluorescent chloroplasts, respectively. The autotrophic category also includes an unknown number of mixotrophic cells. Cell abundance, dimensions, and biovolumes were determined via quasi-automated color image analysis (Verity and Sieracki, 1993; Shopov et al., 2000) equipped with a Photonics Science cooled integrating three-chip color CCD with variable frame rates from 1/10,000 s to 4 min, and an electronic shutter mounted in-line in the microscope lightpath so that the sample was exposed to excitation for only as long as the camera shutter was open. The computer automatically selected random locations on the slide and could return to each location ±1 μm. The commercial driver software (Image Pro Plus v3.0) was customized (Verity et al., 1996; Shopov et al., 2000) so that the entire process (moving to a given location, focusing, opening an electronic shutter, grabbing an image, closing the shutter, and moving to a new location) was automated and computer-controlled.

Table 1
Hydrographic characteristics of the five 24-h stations, with initial stocks of major nutrients, phytoplankton, bacteria, and three groups of microzooplankton (heterotrophic nanoplankton and dinoflagellates, ciliates) in undiluted surface waters used for the dilution experiments

Parameter	24-h station				
	V	IV	III	II	I
Latitude (°N)	78°13.7′	77°40.2′	77°04.3′	75°07.6′	73°48.0′
Longitude (°E)	34°23.0′	34°19.1′	33°49.0′	32°29.2′	31°44.1′
Depth (m)	338	218	172	165	246
Ice cover (%)	0	0	10–20	40–50	70–80
Surface temperature (°C)	7.4	5.3	−0.2	−0.9	−1.6
Surface salinity (PSU)	34.94	35.01	34.79	33.37	33.88
NO_3	6.0	5.0	0.7	1.2	0.1
PO_4	0.5	0.4	0.1	0.1	0.1
$Si(OH)_4$	3.4	3.9	3.6	1.0	1.3
Phytoplankton	36	32	41	52	34
Bacteria	16	18	31	25	18
Het Nano	10	8	8	4	3
Het Dino	4	5	10	9	6
Ciliates	5	9	7	4	3

Nutrient concentrations in μmol l^{-1}. Plankton biomass in μg C l^{-1}.

A minimum of 200 plankton cells of each type and 20 image fields of bacteria (typically 1000 cells) were measured. The average coefficient of variation of triplicate counts of bacteria and nanoplankton was 7% and 13%, respectively. Data were automatically dumped into spreadsheets, and every cell in an image was uniquely identified for post-measurement visual confirmation. Cell biovolume measurements were converted to carbon biomass using conversion factors based on literature values of carbon density of bacteria (350 fgC μm^{-3}: Bjørnsen, 1986) and nano- and microplankton (Verity et al., 1992).

3. Results

Stations I and II were in open ice-free Atlantic waters, Stn. III was in the marginal ice zone (MIZ) with 10–20% ice cover, Stn. IV was in Arctic water with 40–50% ice cover, and Stn. V was also in Arctic water with 70–80% ice cover (Fig. 1). The nutrient conditions and plankton communities reflected both the water mass origin and the extent of ice cover (Table 1). All three stations with ice cover had similar silicate concentrations of 3–4 μM. Stn. V under the most dense ice cover had the highest nitrate and phosphate concentrations of 6.0 and 0.5 μM, respectively. Phytoplankton and bacteria biomass were relatively low at 36 and 16 μgC l^{-1}, respectively; most algal cells were photosynthetic flagellates, with few diatoms or *Phaeocystis pouchetii* colonies. A well-developed, albeit sparse, microbial food web was present, with microzooplankton dominated by 5–20 μm heterotrophic flagellates. Stn. IV with ca. 1:1 ice:open water had somewhat lower nitrate and phosphate concentrations (5.0 and 0.4 μM, respectively), and also had a well developed microbial food web, but dominated in biomass by small (<20 μm) ciliates (Table 1). Again the autotrophic cells were small flagellates, with a preponderance of solitary *P. pouchetii* cells; diatoms and *P. pouchetii* colonies were rare. Stn. III, in the MIZ near the Polar Front had very much reduced nitrate and phosphate levels associated with a much larger sized phytoplankton community, with numerous chained diatoms and *P. pouchetii* colonies. The microbial food web was even more diverse, with similar concentrations of nanoplankton and ciliates but more heterotrophic dinoflagellates (Table 1). A noticeable addition was the colonial mixotroph, *Dinobryon*. In the open Atlantic Stn. II, nitrate and silicate were ca. 1 μM with barely detectable phosphate; among the phytoplankton, chained diatoms and photosynthetic dinoflagellates were

Table 2
Growth and grazing coefficients (±SD), initial chlorophyll *a* biomass (±SD), and grazing impacts calculated from changes in <200 μm chl *a* during the dilution experiments

Dilution experiments: changes in <200 μm chl *a*					
	Stn. V	Stn. IV	Stn. III	Stn. II	Stn. I
k[a]	0.20 (0.03)	0.22 (0.02)	0.28 (0.03)	0.37 (0.04)	0.51 (0.05)
g[b]	0.12 (0.01)	0.18 (0.02)	0.20 (0.02)	0.28 (0.03)	0.41 (0.05)
C_0[c]	0.58 (0.03)	0.44 (0.03)	0.68 (0.05)	0.98 (0.08)	0.63 (0.05)
P_i[d]	13%	20%	22%	32%	50%
P_p[e]	64%	83%	74%	79%	84%

[a] Instantaneous growth coefficient k (day^{-1}).
[b] Instantaneous grazing coefficient g (day^{-1}).
[c] Initial chlorophyll *a* concentration C_0 (μg l^{-1}).
[d] Chl *a* biomass removed daily $P_i(\%day^{-1}) = \frac{(C_0 - C_0 e^g)}{C_0} \times 100$.
[e] Chl *a* production grazed daily $P_p(\%day^{-1}) = \frac{(C_0 e^k - C_0) - (C_0 e^{(k\ g)} - C_0)}{(C_0 e^k - C_0)} \times 100$.

abundant with little *P. pouchetii*. The microzooplankton biomass was reduced and was composed of ca. 50% heterotrophic dinoflagellates, which were larger individuals than at the ice stations. Stn. I, in open Atlantic water far from ice, contained little residual nitrate or phosphate; there were fewer phytoplankton cells of all sizes, primarily a few attenuate pennate diatoms and photosynthetic dinoflagellates. The microbial food web was also reduced, and the dominant microzooplankton were again dinoflagellates (Table 1).

The dilution experiments exhibited distinct patterns among stations and size fractions (Tables 2–4). The <200 μm size fraction initially contained 0.44–0.98 μg chl *a* l^{-1} (Table 2), with the highest concentrations occurring at stations with more abundant diatoms. Comparing Tables 2–4, the <20 μm fraction represented 60%, 57%, 44%, 41%, and 63% of the initial <200 μm chl *a* at Stns. V, IV, III, II, and I, respectively. The <8 μm fraction represented 21%, 23%, 18%, 10%, and 17% of <200 μm biomass, respectively. The smallest contributions by the <20 and <8 μm fractions coincided with the two stations containing the most diatoms.

In the <200 μm fraction (Table 2), phytoplankton growth coefficients were 0.20–0.51 day^{-1} and increased from Stns. V to I. Grazing coefficients were 0.12–0.41 day^{-1} and also increased with decreasing latitude. The percentages of initial phytoplankton biomass removed daily by microzooplankton grazing increased from 13% under the maximum ice cover to 50% in waters furthest from the ice. These grazing rates were equivalent to daily ingestion of 64% to 84% of <200 μm chl *a* production.

In the <20 μm fraction (Table 3), the initial chl *a* biomass was 0.25–0.45 μg l^{-1}. Phytoplankton growth coefficients were 0.26 day^{-1} under substantial ice cover and increased gradually to 0.53 day^{-1} as ice cover was reduced and then disappeared. Grazing coefficients were 0.19–0.46 day^{-1} as increased from Stns. V to I. Microzooplankton grazing rates were equivalent to daily removal of 21% to

Table 3
Growth and grazing coefficients (±SD), initial chlorophyll *a* biomass (±SD), and grazing impacts calculated from changes in <20 μm chl *a* during the dilution experiments

Dilution experiments: changes in <20 μm chl *a*					
	Stn. V	Stn. IV	Stn. III	Stn. II	Stn. I
k[a]	0.26 (0.02)	0.26 (0.03)	0.33 (0.03)	0.38 (0.04)	0.53 (0.06)
g[b]	0.19 (0.01)	0.21 (0.02)	0.25 (0.03)	0.33 (0.03)	0.46 (0.05)
C_0[c]	0.35 (0.03)	0.25 (0.02)	0.30 (0.02)	0.40 (0.02)	0.45 (0.02)
P_i[d]	21%	23%	29%	39%	59%
P_p[e]	74%	81%	87%	89%	90%

[a] Instantaneous growth coefficient k (day^{-1}).
[b] Instantaneous grazing coefficient g (day^{-1}).
[c] Initial chlorophyll *a* concentration C_0 (μg l^{-1}).
[d] Chl *a* biomass removed daily $P_i(\%day^{-1}) = \frac{(C_0 - C_0e^g)}{C_0} \times 100$.
[e] Chl *a* production grazed daily $P_p(\%day^{-1}) = \frac{(C_0e^k - C_0) - (C_0e^{(k\ g)} - C_0)}{(C_0e^k - C_0)} \times 100$.

Table 4
Growth and grazing coefficients (±SD), initial chlorophyll *a* biomass (±SD), and grazing impacts calculated from changes in <8 μm chl *a* during the dilution experiments

Dilution experiments: changes in <8 μm chl *a*					
	Stn. V	Stn. IV	Stn. III	Stn. II	Stn. I
k[a]	0.27 (0.03)	0.27 (0.01)	0.32 (0.02)	0.41 (0.04)	0.53 (0.05)
g[b]	0.23 (0.02)	0.24 (0.03)	0.29 (0.03)	0.38 (0.03)	0.51 (0.05)
C_0[c]	0.12 (0.01)	0.10 (0.01)	0.12 (0.01)	0.10 (0.01)	0.09 (0.01)
P_i[d]	26%	27%	34%	47%	67%
P_p[e]	86%	91%	91%	94%	97%

[a] Instantaneous growth coefficient k (day^{-1}).
[b] Instantaneous grazing coefficient g (day^{-1}).
[c] Initial chlorophyll *a* concentration C_0 (μg l^{-1}).
[d] Chl *a* biomass removed daily $P_i(\%day^{-1}) = \frac{(C_0 - C_0e^g)}{C_0} \times 100$.
[e] Chl *a* production grazed daily $P_p(\%day^{-1}) = \frac{(C_0e^k - C_0) - (C_0e^{(k\ g)} - C_0)}{(C_0e^k - C_0)} \times 100$.

Table 5
Mean (±SD) growth and grazing coefficients, initial chl *a* biomass, and grazing impacts averaged for the five 24-h stations for each of three size fractions of chl *a*

Barents Sea dilution experiments					
	k[a]	g[b]	C_0[c]	P_i[d]	P_p[e]
<200	0.32 ± 0.13	0.24 ± 0.10	0.66 ± 0.20	35 ± 15	77 ± 8
<20	0.35 ± 0.11	0.29 ± 0.13	0.35 ± 0.08	34 ± 16	84 ± 7
<8	0.36 ± 0.11	0.33 ± 0.11	0.11 ± 0.01	40 ± 17	92 ± 4

[a] Instantaneous growth coefficient k (day^{-1}).
[b] Instantaneous grazing coefficient g (day^{-1}).
[c] Initial chlorophyll *a* concentration C_0 (μg l^{-1}).
[d] Chl *a* biomass removed daily $P_i(\%day^{-1}) = \frac{(C_0 - C_0e^g)}{C_0} \times 100$.
[e] Chl *a* production grazed daily $P_p(\%day^{-1}) = \frac{(C_0e^k - C_0) - (C_0e^{(k\ g)} - C_0)}{(C_0e^k - C_0)} \times 100$.

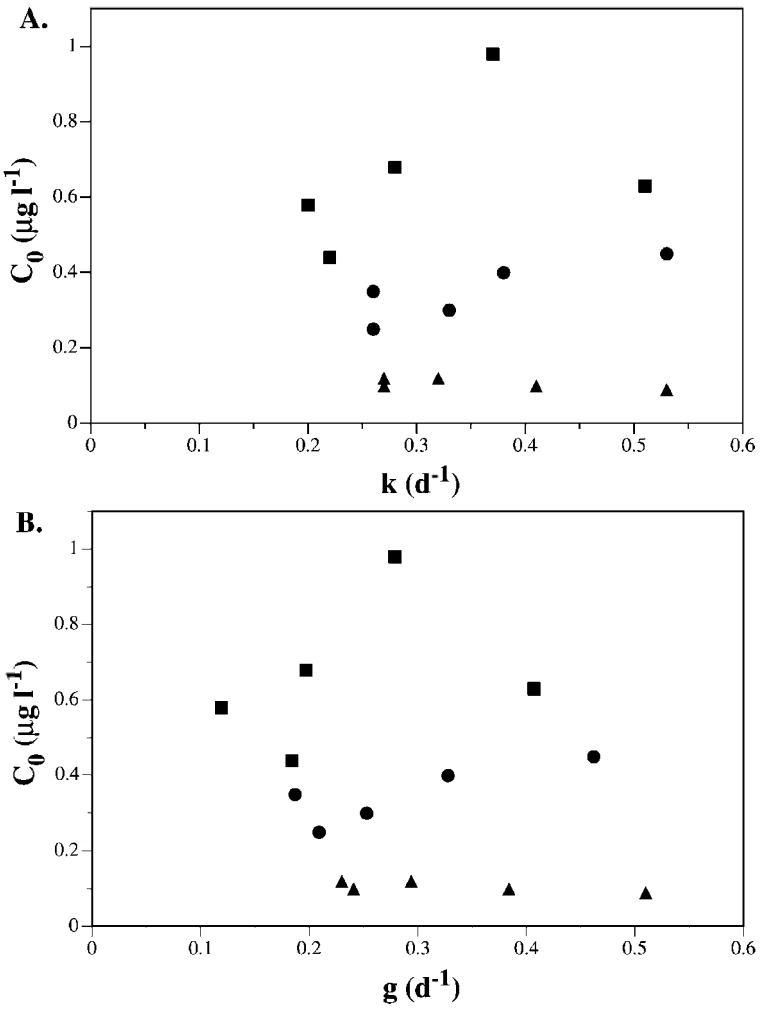

Fig. 2. (A) Relationship between chlorophyll *a* standing stock (C_0) and the experimentally determined instantaneous growth coefficient (k) in the <200 µm fraction (■), <20 µm fraction (●), and <8 µm fraction (▲). (B) Relationship between chlorophyll *a* standing stock (C_0) and the experimentally determined instantaneous grazing coefficient (g). Symbols as in panel A.

59% of <20 µm chl *a* standing stocks, or 74% to 90% of measured daily <20 µm chl *a* production. Both parameters increased with decreasing latitude.

In the <8 µm fraction (Table 4), initial pigment concentrations were similar (0.09–0.12 µg l^{-1}) at all five stations. Algal growth coefficients were similar (0.27 day^{-1}) at the two stations with the heaviest ice cover, and increased with distance away from the ice to 0.53 day^{-1} at Stn. I. Microzooplankton grazing coefficients were 0.23–0.51 day^{-1} and showed the same spatial pattern as algal growth. Grazing rates were equivalent to daily removal of 26% to 67% of initial <8 µm algal biomass, or 86% to 97% of <8 µm chl *a* production, with the highest removal in open waters.

General trends were apparent with respect to phytoplankton cell size when experimental data for all stations were combined (Table 5). Growth and grazing coefficients increased with decreasing cell size category although differences were not significant due in inter-station variability. The <20 and <8 µm fractions averaged 53% and 20% of <200 µm initial chl *a* stocks; these concentrations were significantly different from one another. The mean percentage of initial

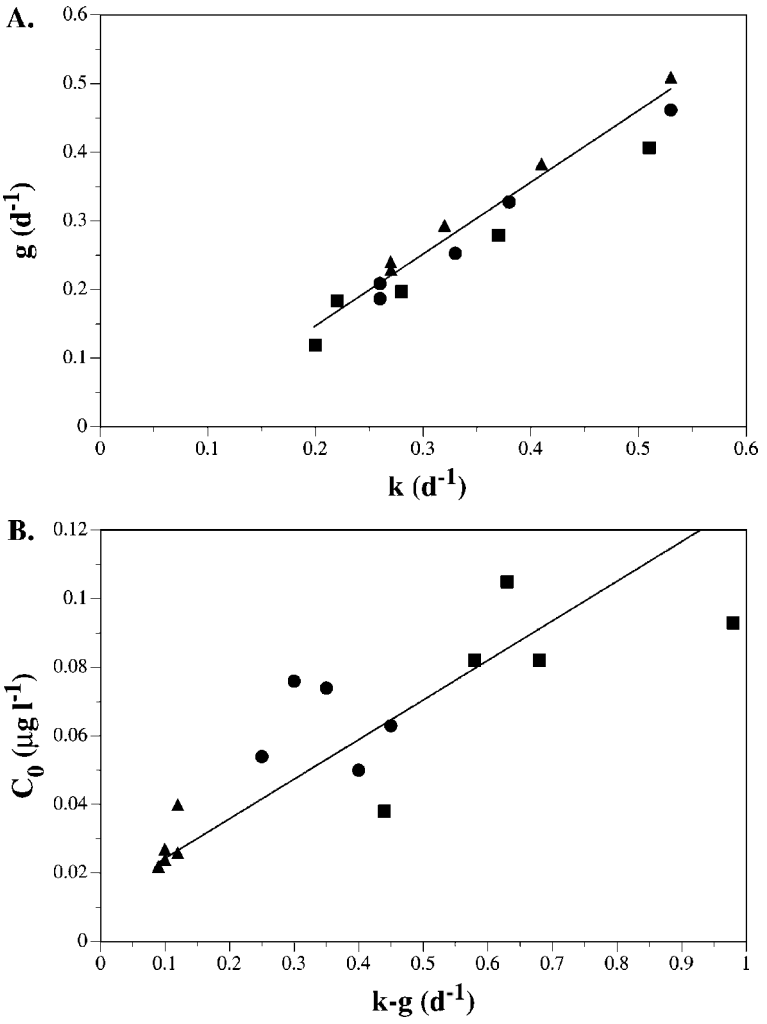

Fig. 3. (A) Relationship between the experimentally determined instantaneous growth coefficient (k) and grazing coefficient (g). Regression model: g (day^{-1}) = 0.99 [k (day^{-1})] – 0.05, r^2 = 0.94, df = 14, P < 0.0001. (B) Relationship between chlorophyll a standing stock (C_0) and the net difference in growth and grazing coefficients. Regression model: C_0 = 7.6 [$k - g$ (day^{-1})] – 0.06, r^2 = 0.64, df = 14, P < 0.0003. All symbols as in Fig. 2.

chl a stocks removed daily by microzooplankton was greater in the < 8 μm class than in larger size classes, but the differences were not significant. Mean daily algal production lost to grazing was 77% (< 200 μm), 84% (< 20 μm), and 92% (< 8 μm); < 8 μm production grazed was significantly greater than < 200 μm production grazed.

The standing stocks of phytoplankton in all size classes varied with growth and grazing coefficients (Fig. 2). Higher chl a biomass was generally associated with higher growth coefficients in the < 200 and < 20 μm size classes (Fig. 2A), but trends were not significant; < 8 μm biomass did not vary with growth coefficient. Considering all three size classes, there was no relationship apparent between standing stocks and growth coefficients. Likewise, higher chl a concentrations were also associated with higher grazing coefficients in the two largest size fractions but not in the < 8 μm category (Fig. 2B); again, however, differences were not significant due to the low number of

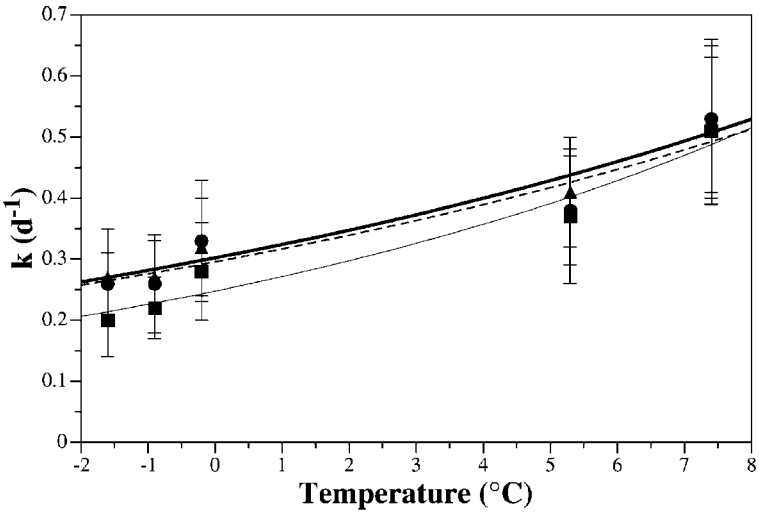

Fig. 4. Relationship between phytoplankton growth coefficient (k) in three size fractions, and surface water temperature (T) at the five stations. Regression models: <200 μm chl: k (day^{-1})=0.248e$^{(0.092 \times T)}$, r^2=0.94, n=5, P(intercept)<0.007, P(slope)<0.006. <20 μm chl: k (day^{-1})=0.295e$^{(0.069 \times T)}$, r^2=0.89, n=5, P(intercept)<0.0002, P(slope)<0.07. <8 μm chl: k (day^{-1})=0.302e$^{(0.070 \times T)}$, r^2=0.96, n=5, P(intercept)<0.0001, P(slope)<0.004. All size fractions combined: k (day^{-1})=0.281e$^{(0.077 \times T)}$, r^2=0.96, n=15, P(intercept)<0.0001, P(slope)<0.0001. <200 μm fraction: (■) and solid line. <20 μm fraction: (●) and dashed line. <8 μm fraction: (▲) and bold line.

data points in each size class. Combining all three size categories, there was no relationship between algal biomass and grazing coefficients.

Algal growth and microzooplankton grazing coefficients were not correlated within a given size class, but across the various size categories there was a

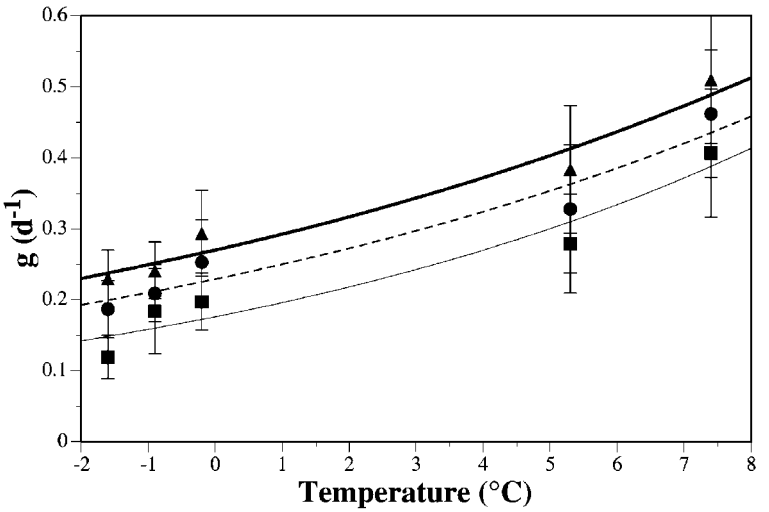

Fig. 5. Relationship between microzooplankton grazing coefficient (g) in three size fractions, and surface water temperature (T) at the five stations. Regression models: <200 μm chl: g (day^{-1})=0.176e$^{(0.107 \times T)}$, r^2=0.88, n=5, P(intercept)<0.0003, P(slope)<0.02. <20 μm chl: g (day^{-1})=0.229e$^{(0.087 \times T)}$, r^2=0.94, n=5, P(intercept)<0.0001, P(slope)<0.06. <8 μm chl: g (day^{-1})=0.270e$^{(0.080 \times T)}$, r^2=0.96, n=5, P(intercept)<0.0001, P(slope)<0.004. All size fractions combined: g (day^{-1})=0.221e$^{(0.091 \times T)}$, r^2=0.76, n=15, P(intercept)<0.0001, P(slope)<0.0001. Symbols and lines as in Fig. 4.

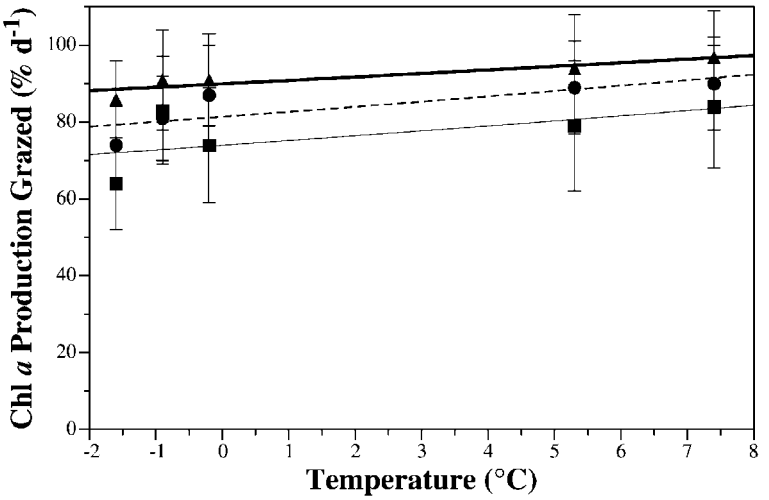

Fig. 6. Relationship between the percentage of daily chl *a* production grazed by microzooplankton in three size fractions, and surface water temperature at the five stations. Regression models: <200 μm chl: P_p (%day^{-1}) = 73.96e$^{(0.016 \times T)}$, $r^2 = 0.36$, $n = 5$, P(intercept) < 0.0001, P(slope) < 0.28. <20 μm chl: P_p (%day^{-1}) = 81.37e$^{(0.016 \times T)}$, $r^2 = 0.62$, $n = 5$, P(intercept) < 0.0001, P(slope) < 0.11. <8 μm chl: P_p (%day^{-1}) = 89.93e$^{(0.010 \times T)}$, $r^2 = 0.81$, $n = 5$, P(intercept) < 0.0001, P(slope) < 0.04. All size fractions combined: P_p (%day^{-1}) = 81.49e$^{(0.014 \times T)}$, $r^2 = 0.25$, $n = 15$, P(intercept) < 0.0001, P(slope) < 0.07. Symbols and lines as in Fig. 4.

significant linear relationship (Fig. 3A): variations in algal growth rates explained 94% of the variance in microzooplankton grazing. Within a given size class, the difference between growth and grazing was not strongly related to algal biomass (Fig. 3B). However, combining size classes, ca. 2/3 of the variance in chl *a* standing stocks was explained by the difference between algal growth and grazing losses.

There was a 9 °C range in surface water temperatures across the five stations. Phytoplankton growth coefficients in all three size classes were positively correlated with temperature (Fig. 4). Fits to exponential regression models yielded generally highly significant regression coefficients. Data from the three size fractions were not log transformed because Kolmogorov–Smirnov tests indicated the data were normally distributed (P>0.05: StatView v5.0, SAS Institute). The slope of the regression for each size fraction was equivalent to Q_{10}'s of 2.5 (<200 μm) and 2.0 (<20 and <8 μm); for all size classes combined the slope was equivalent to a Q_{10} of 2.2. Microzooplankton grazing coefficients also exhibited a positive relationship with temperature (Fig. 5). Exponential regression model coefficients were somewhat lower than those for growth, but generally also highly significant. The slope of the regression for each size fraction was equivalent to Q_{10}'s of 2.9 (<200 μm), 2.4 (<20 μm), and 2.2 (<8 μm); for all size classes combined the slope was equivalent to a Q_{10} of 2.5. The fraction of chl *a* production grazed daily by microzooplankton also increased with temperature (Fig. 6). Exponential fits for each size fraction had poorer regression coefficients for the equation slopes. The slope of the regression for each size fraction was equivalent to Q_{10}'s of 1.2 (<200 and <20 μm) and 1.1 (<8 μm); for all size classes combined the slope was equivalent to a Q_{10} of 1.2.

4. Discussion

4.1. Hydrography and plankton development

The general hydrography, nutrients, and plankton distribution in 1999 reflected the zonal structure reported for the central Barents Sea in late spring (Loeng et al., 1997; Wassmann et al., 1999b). The station locations here were selected based upon that stratigraphy and prior emphasis (Skjoldal et al., 1987; Wassmann and Slagstad, 1993; Hansen et al., 1996;

Wassmann et al., 1999b). Typically, moving south–north one crosses the Norwegian Coastal Current, Atlantic water, the Polar Front, the marginal ice zone, and into Arctic water under the ice. There are also lateral meanders of the Polar Front which inject east–west variability. Movements and interactions among these water masses creates a "sandwich-like" structure (Wassmann et al., 1999b) whereby contrasting stages of spring bloom development occur. These authors posit that the spring bloom proceeds both north and south in two waves. The beginning of the spring bloom propagates north–south from the MIZ into Atlantic water and is regulated by the gradually reducing vertical mixing. In the other wave, the mature phase of the bloom propagates as a narrow band south–north as the ice edge retreats, and is caused by increased stratification due to ice melt and increased insolation. Ice and wind strongly impact productivity of the Barents Sea (Sakshaug and Slagstad, 1992). More details on hydrography and circulation in 1999 are given in Reigstad et al. (2002, this issue) and Kaltin et al. (2002, this issue).

The five stations studied here in June/July represented the following water masses. Stns. V and IV were in Arctic waters, and ca. half of their typical winter-time nutrient loads (12 μM nitrate, 5 μM silicate, and 0.9 μM phosphate: Wassmann et al., 1999b) had already been assimilated by phytoplankton and bacteria (see also Allen et al., 2002, this issue). However, there were still adequate macronutrients remaining to fuel continued production (Table 1). Stn. III was in the MIZ: surface nitrate concentrations had been strongly reduced relative to silicate, implying significant prior utilization by phytoflagellates and incipient nitrate and/or phosphate limitation. Stations II and I were in Atlantic waters, and both exhibited signs of being in post-bloom conditions. Stn. II contained low but equimolar concentrations of nitrate and silicate, suggesting significant utilization by diatoms and incipient silicate limitation. At Stn. I, nitrate and phosphate were almost undetectable, while silicate remained at ca. 1 μM, similar to that at Stn. II. This scenario is consistent with the observed distribution of high diatom and *P. pouchetii* biomass at Stn. III, lower but still dominant contributions by diatoms at Stn. II, and their replacement by flagellates at Stn. I. It also supports the theory that the spatial distribution of phytoplankton development mimics the temporal pattern, e.g. early stages in the north and later stages in the south. A similar spatial pattern in nutrients and phytoplankton was found in the early summer of 1991 (Owrid et al., 2000).

4.2. Food web structure and microzooplankton grazing

The spring bloom development in north polar waters typically begins with small-celled phytoflagellates at low concentrations, progresses into a mature phase dominated by large cells, e.g. diatoms and *P. pouchetii* colonies, and then terminates in a reduced biomass of flagellated cells (Sakshaug and Skjoldal, 1989). Small flagellates are present during the high biomass mature phase but were thought to have only small relative contributions (Slagstad and Wassmann, 1997). However, the present data indicate that this is not always the case. A significant fraction of the surface microphytoplankton (<200 μm) was composed of nanoplankton (<20 μm), with an average of 53% over the five stations (data from Tables 2–4). A mean of 18% of the chl *a* also passed through 8 μm mesh, so that an average of 35% of chl *a* was in the 8–20 μm size fraction. The small fractions contributed least at the two stations with more abundant diatoms. This scenario of relatively significant contributions by nanoplankton was also observed in this same region in 1993 (Wassmann et al., 1999b; Jensen and Hansen, 2000). In March 1998, small cells were also predominant although this was prior to vernal bloom development (Ratkova and Wassmann, 2002, this issue). In May 1998, *P. pouchetii* colonies were overwhelming abundant during peak bloom periods (Ratkova and Wassmann, 2002, this issue).

Phytoplankton cells contributed the largest proportions of total microplankton biomass (Table 1); the biomass of bacteria (total DAPI-stained cells) was generally ca. 1/2 to 2/3 that of phytoplankton. The total biomass of the three major microzooplankton groups (heterotrophic nanoflagellates, dinoflagellates, ciliates) exceeded that of bacteria under the ice, but was less in the MIZ and open Atlantic waters. The three groups exhibited spatial patterns in their peak distributions: nanoflagellates under the ice, dinoflagellates coincident with diatoms, and ciliates in the MIZ. The combined heterotrophic biomass generally mimicked that of phytoplankton. The general features

of the spatial distribution of heterotrophs agree with that reported by Hansen et al. (1996) and Jensen and Hansen (2000) for these waters in May 1993, although the latter biomasses were often higher, reflecting the peak vernal development at that time.

Microzooplankton were active grazers on the microphytoplankton community, and likely also on bacteria (Tables 2–5). Phytoplankton growth rates in surface waters, measured as chl *a* production, were 0.2 to 0.5 day^{-1} in all size fractions, with the highest rates occurring at the more southern stations. There was not a strong size-class dependence in growth coefficients. These growth coefficients are in the range observed for maximum growth rates observed in culture for various diatoms isolated from the Barents Sea (Gilstad and Sakshaug, 1990). Grazing rates ranged from 0.1 to 0.5 day^{-1}, with the highest rates also occurring in more southern stations. These grazing rates compare favorably with microzooplankton growth rates measured in these waters in May 1993 (Hansen and Jensen, 2000). While not significantly different across stations, there was a trend for average grazing rates to be higher on smaller size classes of phytoplankton. The fraction of daily chl *a* production ingested by microzooplankton exhibited a broad range from 64% (Stn. V, <200 μm fraction) to 97% (Stn. I, <8 μm fraction). Higher grazing losses were observed in smaller size classes and, independent of size, at more southern stations. Mean daily removal of surface primary production was 77% (<200 μm), 84% (<20 μm), and 92% (<8 μm). These data indicate that the fate of large fractions of daily primary production was to be channeled through microzooplankton. Similar conclusions were drawn during early bloom development (Hansen et al., 1996).

By definition, the standing stock of a pelagic trophic group reflects the net difference between inputs (e.g. growth, immigration) and losses (grazing, lysis, apoptosis, sedimentation, advection). For phytoplankton, the dominant processes are thought to be in situ growth, grazing, and sedimentation. The standing stocks of microphytoplankton observed in surface waters of the Barents Sea in July 1999 were not solely related to only growth or grazing processes (Fig. 2). For larger size classes, there tended to be a weak positive relationship between either rate and the observed standing stock. This makes intuitive sense for growth but not for grazing. The latter correlation appears to be coincidental due to the strong positive dependence of grazing on growth coefficients (Fig. 3A). But phytoplankton biomass (measured as chl *a*) could be predicted with considerable accuracy from the net difference between growth and grazing (Fig. 3B). This supports the notion that, for micro- and nanophytoplankton, these two processes strongly influenced near-surface distributions. A similar relationship was observed in Narragansett Bay, RI, a temperate estuary where grazing removal of chl *a* production at low temperatures was also quite high (60–90% day^{-1}: Verity, 1986a).

At least part of the explanation for these relationships may be the temperature dependence of metabolic rates. Both phytoplankton growth coefficients and microzooplankton grazing coefficients, in all three size fractions, exhibited consistent increases with water temperature (Figs. 4–6). These were fit to exponential regression models which imply Q_{10}'s of ca. 2.0–2.5 for growth and 2.2–2.9 for grazing. These Q_{10}'s are not very different from those reported for auto- and heterotrophic micro- and nanoplankton in culture (Stoecker et al., 1983; Verity, 1985; Suzuki and Takahashi, 1995; and citations therein). Chl *a* growth rates in Narragansett Bay exhibited a Q_{10} of 1.7 (Verity, 1986a), while growth rates of tintinnid ciliates had a Q_{10} of 1.8 (Verity, 1986b). The lower Q_{10} (1.1–1.2) for the percentage of daily production lost to grazing in the Barents Sea likely reflects the small difference between Q_{10}'s for growth and grazing. It is interesting to note that the fraction of chl *a* production ingested by microzooplankton increased with temperature in temperate shelf waters as well (Verity et al., in press). A strong dependence of microzooplankton grazing on temperature was also observed in the open northeastern Atlantic Ocean (Burkill et al., 1993).

If ingestion by primarily protozoan grazers is the major fate of microphytoplankton production, then little else is available to meet other demises. This implies that, at least in surface waters during early summer, grazing by mesozooplankton and direct sedimentation are of little consequence for this size class of phytoplankton. A similar conclusion about the role of mesozooplankton in the grazing of primary production was drawn by Hansen et al. (1996) for these waters in spring. Microzooplankton grazing was

reported to be more important than mesozooplankton grazing in retaining nutrients and organic matter in the upper water column in the Barents Sea in spring (Andreassen and Wassmann, 1998). It may be that, except during the peak of the vernal bloom, microzooplankton are a major food source for mesozooplankton in the Barents Sea. Similar conclusions were reached for the north Norwegian shelf for most of the year (Verity et al., 1999; Wassmann et al., 1999a), and the importance of top-down influences on community structure and ecosystem function may be a general feature of these waters (Wassmann, 2001). Also supporting this theory are the direct measurements of phytoplankton sedimentation during this cruise, which showed little vertical export of chl *a* (Olli et al., 2002, this issue), implying retention in the upper water column, as described previously in the Barents Sea in other years (Wassmann, 2001).

4.3. A re-evaluation of arctic marine pelagic food-webs

When larger zooplankton forms such as *Calanus* spp. ascend to the surface layers in spring, they have to make use of the short period of phytoplankton abundance in the Arctic, giving rise to new generations and storing energy depots. The copious blooms of large phytoplankton cells in the Arctic were historically interpreted that these cells were the base for the rich growth of mesozooplankton, which in turn fed abundant stocks of fish, birds, and mammals. Recent investigations, however, indicate that feeding, growth and development of the pivotal taxon *Calanus* appears only weakly associated with the abundance of large phytoplankton (Kleppel et al., 1991, 1998; Ohman and Runge, 1994; Runge and Plourde, 1996). Small-sized algae can be successfully be ingested by *C. finmarchicus* (Båmstedt et al., 1999). Microzooplankton are usually assumed to feed on flagellates (Hansen et al., 1993), but observations on diatom grazing have also been reported (Hansen et al., 1996; Nejstgaard et al., 1997). The significance of protozoan grazers for the fate of microplankton described here, the large fraction of small phytoplankton cells (e.g. Ratkova and Wassmann, 2002, this issue) and the high biomass and growth of mesozooplankton in the Barents Sea (e.g. Skjoldal et al., 1987; Arashkevich et al., 2002, this issue) all suggest an effective link between new nutrients, the microbial food web and the classical food web, creating one of the world's most productive fishing grounds. Mesozooplankton graze extensively on large phytoplankton cells, but they also supplement their food demand by grazing on detritus and protozoa. It is posited here that they draw a major fraction of their demands of nutrients and energy through a microbial food web shunt to sustain their populations during late spring (Hansen et al., 1996) and summer (this investigation) in the Barents Sea. This also implies that mesozooplankton depend on the utilization of rich protozooplankton growth and are thus more omnivorous in situ rather than herbivorous as previously assumed (Wassmann, 2001). If generally applicable, the present and recent literature data suggest that the general conceptual notion that the Arctic food webs are short and lead directly to macroconsumers may need re-evaluation.

Acknowledgements

The authors wish to thank S. Øeygarden, C. Wexels Riser, and M. Reigstad for their tremendous efforts in preparation for the cruise, and J. Greig for analyzing samples afterwards. We further acknowledge the captain and crew of R/V Jan Mayen for support activities. This research was supported by NSF grants OCE-95-21086 and 99-82133 and DOE grant FG-02-98ER62531. D. Peterson prepared the manuscript and A. Boyette drafted the figures.

References

Allen, A.E., Howard-Jones, M.H., Frischer, M.E., Verity, P.G., Bronk, D.A., Sanderson, M.P., Booth, M.G., 2002. Importance of heterotrophic bacterial assimilation of ammonium and nitrate in the Barents Sea during summer. J. Mar. Syst., this issue.

Andreassen, I.J., Wassmann, P., 1998. Vertical flux of phytoplankton and particulate biogenic matter in the marginal ice zone of the Barents Sea in May 1993. Mar. Ecol. Prog. Ser. 170, 1–14.

Arashkevich, E., Wassmann, P., Pasternak, A., Wexels Riser, C., 2002. Seasonal and spatial changes in biomass, structure, and development progress of the zooplankton community in the Barents Sea. J. Mar. Syst., this issue.

Archer, S.D., Verity, P.G., Stefels, J., 2000. Impact of microzooplankton on the progression and fate of the spring bloom in fjords of northern Norway. Aquat. Microb. Ecol. 22, 27–41.

Azam, F., Fenchel, T., Field, J.G., Gray, J.S., Meyer-Reil, L.A.,

Thingstad, F., 1983. The ecological role of water-column microbes in the sea. Mar. Ecol. Prog. Ser. 10, 257–263.

Båmstedt, U., Nejstgaard, J.C., Solberg, P.T., 1999. Utilization of small-sized food algae by *Calanus finmarchicus* (Copepoda: Calanoida) and the significance of feeding history. Sarsia 84, 19–38.

Bjørnsen, P.K., 1986. Automatic determination of bacterioplankton biomass by image analysis. Appl. Environ. Microbiol. 51, 1199–1204.

Burkill, P.H., Edwards, E.S., John, A.W.G., Sleigh, M.A., 1993. Microzooplankton and their herbivorous activity in the northeastern Atlantic Ocean. Deep-Sea Res., Part II 40, 479–493.

Føyn, L., Magnussen, M., Seglem, K., 1981. Automatic analysis of nutrients with on-line data treatment. A presentation of the construction and performance of the system in use on Institute of Marine Research vessels and in the laboratory. Fisken Havet, B 4, 1–40 (in Norwegian).

Gallegos, C.L., 1989. Microzooplankton grazing on phytoplankton in the Rhode River, Maryland: nonlinear feeding kinetics. Mar. Ecol. Prog. Ser. 57, 23–33.

Gifford, D.J., 1988. Impact of grazing by microzooplankton in the Northwest Arm of Halifax Harbour, Nova Scotia. Mar. Ecol. Prog. Ser. 47, 249–258.

Gilstad, M., Sakshaug, E., 1990. Growth rates of ten diatom species from the Barents Sea at different irradiances and day lengths. Mar. Ecol. Prog. Ser. 64, 169–173.

Gran, H.H., 1902. Das plankton des Norwegischen Nordmeeres. Report on Norwegian Fishery and Marine Investigations, vol. II, No. 5, 222 pp.

Hansen, B.W., Jensen, F., 2000. Specific growth rates of protozooplankton in the marginal ice zone of the central Barents Sea during spring. J. Mar. Biol. Assoc. U.K. 80, 37–44.

Hansen, F.C., Reckermann, M., Klein Breteler, W.C.M., Riegman, R., 1993. *Phaeocystis* blooming enhanced by copepod predation on protozoa: evidence from incubation experiments. Mar. Ecol. Prog. Ser. 102, 51–57.

Hansen, B., Christiansen, S., Pedersen, G., 1996. Plankton dynamics in the Marginal Ice Zone of the central Barents Sea during spring: carbon flow and structure of the grazer food chain. Polar Biol. 16, 115–128.

Howard-Jones, M.H., Ballard, V.D., Allen, A.E., Frischer, M.E., Verity, P.G., 2002. Distribution of bacterial biomass and activity in the marginal ice zone of the central Barents Sea during summer. J. Mar. Syst., this issue.

Jensen, F., Hansen, B.W., 2000. Ciliates and heterotrophic dinoflagellates in the marginal ice zone of the central Barents Sea during spring. J. Mar. Biol. Assoc. U.K. 80, 45–54.

Kaltin, S., Anderson, L.G., Olsson, K., Fransson, A., Chierici, M., 2002. Uptake of atmospheric carbon dioxide in the Barents Sea. J. Mar. Syst., this issue.

Kleppel, G.S., Holliday, D.V., Pieper, R.E., 1991. Trophic interactions between copepods and microplankton: a question about the role of diatoms. Limnol. Oceanogr. 36, 172–178.

Kleppel, G.S., Burkart, C.A., Houchin, L., 1998. Nutrition and the regulation of egg production in the calanoid copepod *Acartia tonsa*. Limnol. Oceanogr. 43, 1000–1007.

Landry, M.R., 1993. Estimating rates of growth and grazing mortality of phytoplankton by the dilution method. In: Kemp, P.F., Sherr, B.F., Sherr, E.B., Cole, J.J. (Eds.), Handbook of Methods in Aquatic Microbial Ecology. Lewis, New York, pp. 715–722.

Landry, M.R., Hassett, R.P., 1982. Estimating the grazing impact of marine microzooplankton. Mar. Biol. 67, 283–288.

Levinsen, H., Nielsen, T.G., Hansen, B.W., 2000. Annual succession of marine protozoans in the arctic with emphasis on winter dynamics. Mar. Ecol. Prog. Ser. 206, 119–134.

Loeng, H., Ozhigin, V., Ådlandsvik, B., 1997. Water fluxes through the Barents Sea. ICES J. Mar. Sci. 54, 310–317.

Lohmann, H., 1908. Untersuchungen zur Festellung des vollständigen Gehaltes des Meeres an Plankton. Wiss. Meeresunters., Abt. Kiel, N.F. 10, 129–370.

Nejstgaard, J.C., Gismervik, I., Solberg, P.T., 1997. Feeding and reproduction by *Calanus finmarchicus*, and microzooplankton grazing during mesocosm blooms of diatoms and the coccolithophore *Emiliania huxleyi*. Mar. Ecol. Prog. Ser. 147, 197–217.

Nielsen, T.G., Hansen, B.W., 1999. Plankton community structure and carbon cycling on the western coast of Greenland during the stratified summer situation: I. Hydrography, phytoplankton and bacterioplankton. Aquat. Microb. Ecol. 16 (3), 205–216.

Ohman, M.D., Runge, J.A., 1994. Sustained fecundity when phytoplankton resources are in short supply: omnivory by *Calanus finmarchicus* in the Gulf of St. Lawrence. Limnol. Oceanogr. 39, 21–36.

Olli, K., Wexels Riser, C., Wassmann, P., Ratkova, T., Arashkevich, E., Pasternak, A., 2002. Seasonal variation in vertical flux of biogenic matter in the marginal ice zone and the central Barents Sea. J. Mar. Syst., this issue.

Owrid, G., Socal, G., Civitarese, G., Luchetta, A., Wiktor, J., Nothig, E.-M., Andreassen, I., Schauer, U., Strass, V., 2000. Spatial variability of phytoplankton, nutrients, and new production estimates in the waters around Svalbard. Polar Res. 19, 155–171.

Pomeroy, L.R., 1974. The ocean's food web, a changing paradigm. BioScience 24, 499–504.

Ratkova, T., Wassmann, P., 2002. Seasonal variation and spatial distribution of phyto- and protozooplankton in the central Barents Sea. J. Mar. Syst., this issue.

Reigstad, M., Wassmann, P., Wexels Riser, C., Øeygarden, S., Rey, F., 2002. Variations in hydrography, nutrients, and chlorophyll *a* in the marginal ice zone and the central Barents Sea. J. Mar. Syst., this issue.

Rey, F., Loeng, H., 1985. The influence of ice and hydrographic conditions on the development of phytoplankton in the Barents Sea. In: Gray, J.S., Christiansen, M.E. (Eds.), Marine Biology of Polar Regions and Effects of Stress on Marine Organisms. Wiley, New York, NY, pp. 49–63.

Runge, J.A., Plourde, S., 1996. Fecundity characteristics of *Calanus finmarchicus* in coastal waters of eastern Canada. Ophelia 44, 171–187.

Sakshaug, E., 1991. Food webs and primary production in the Barents SeaProc. NIPR Symp. Polar Biol. Tokyo, vol. 4, pp. 1–8.

Sakshaug, E., Skjoldal, H.R., 1989. Life at the ice edge. Ambio 18, 60–67.

Sakshaug, E., Slagstad, D., 1992. Sea ice and wind: effects on

primary productivity in the Barents Sea. Atmos.-Ocean 30, 579–591.

Shopov, A., Williams, S.C., Verity, P.G., 2000. Improvements in image analysis and fluorescence microscopy to discriminate and enumerate bacteria and viruses in aquatic samples. Aquat. Microb. Ecol. 22, 103–110.

Skjoldal, H.R., Hassel, A., Rey, F., Loeng, H., 1987. Spring phytoplankton development and zooplankton reproduction in the central Barents Sea in the period 1979–1984. In: Loeng, H. (Ed.), The Effect of Oceanographic Conditions on Distribution and Population Dynamics of Commercial Fish Stocks in the Barents Sea, Proceedings of the 3rd Soviet–Norwegian Symposium. Inst. Mar. Res., Bergen, pp. 59–89.

Slagstad, D., Wassmann, P., 1997. Climate forcing and carbon flux in the Barents Sea: 3D simulations of ice distribution, primary production, and vertical export of particulate organic matter. Mem. Natl. Inst. Polar Res., Spec. Issue 51, 119–141.

Stoecker, D., Davis, L.H., Provan, A., 1983. Growth of *Favella* sp. (Ciliata: Tintinnina) and other microzooplankton in cages incubated in situ and comparison to growth in vitro. Mar. Biol. 75, 293–302.

Stoecker, D.K., Putt, M., Moisan, T., 1995. Nano- and microplankton dynamics during the spring *Phaeocystis pouchetii* bloom in McMurdo Sound, Antarctica. J. Mar. Biol. Assoc. U.K. 75, 815–832.

Strickland, J.D.H., Parsons, T.R., 1972. A practical handbook of seawater analysis. Bull. Fish. Res. Board Can. 167, 1–310.

Suzuki, Y., Takahashi, M., 1995. Growth responses of several diatom species isolated from various environments to temperature. J. Phycol. 31, 880–888.

Verity, P.G., 1985. Grazing, respiration, excretion, and growth of tintinnids. Limnol. Oceanogr. 30, 1268–1828.

Verity, P.G., 1986a. Grazing of phototrophic nanoplankton by microzooplankton in Narragansett Bay. Mar. Ecol. Prog. Ser. 29, 105–115.

Verity, P.G., 1986b. Growth rates of natural tintinnid populations in Narragansett Bay. Mar. Ecol. Prog. Ser. 29, 117–126.

Verity, P.G., Sieracki, M.E., 1993. Use of color image analysis and epifluorescence microscopy to measure plankton biomass. In: Kemp, P.F., Sherr, B.F., Sherr, E.B., Cole, J.J. (Eds.), Handbook of Methods in Aquatic Microbial Ecology. Lewis, New York, pp. 327–338.

Verity, P.G., Smetacek, V., 1996. Organism life cycles, predation, and the structure of marine pelagic ecosystems. Mar. Ecol. Prog. Ser. 130, 277–293.

Verity, P.G., Vernet, M., 1992. Microzooplankton grazing, pigments and composition of plankton communities during the late spring in two Norwegian fjords. Sarsia 77, 263–274.

Verity, P.G., Redalje, D.G., Lohrenz, S.E., Flagg, C., Hristov, R., in press. Coupling between primary production and pelagic consumption in a temperate ocean margin pelagic ecosystem. Deep-Sea Res., Part II.

Verity, P.G., Robertson, C.Y., Tronzo, C.R., Andrews, M.G., Nelson, J.R., Sieracki, M.E., 1992. Relationship between cell volume and the carbon and nitrogen content of marine photosynthetic nanoplankton. Limnol. Oceanogr. 37, 1434–1446.

Verity, P.G., Stoecker, D.K., Sieracki, M.E., Nelson, J.R., 1996. Microzooplankton grazing of primary production at 140 W in the equatorial Pacific. Deep-Sea Res., Part II 43, 1227–1255.

Verity, P.G., Wassmann, P., Ratkova, T.N., Andreassen, I.J., Nordby, E., 1999. Seasonal patterns in composition and biomass of autotrophic and heterotrophic nano- and microplankton communities on the north Norwegian shelf. Sarsia 84, 265–277.

Wassmann, P., 2001. Vernal export and retention of biogenic matter in the northeastern North Atlantic and adjacent Arctic Ocean: the role of the Norwegian Atlantic Current and topography. Mem. Natl. Inst. Polar Res., Spec. Issue 54, 377–392.

Wassmann, P., 2002. Seasonal C-cycling variability in the open and ice-covered waters of the Barents Sea: an introduction. J. Mar. Syst., this issue.

Wassmann, P., Slagstad, D., 1993. Seasonal and interannual dynamics of carbon flux in the Barents Sea: a model approach. Polar Biol. 13, 363–372.

Wassmann, P., Vernet, M., Mitchell, B.G., Rey, F., 1990. Mass sedimentation of *Phaeocystis pouchetii* in the Barents Sea. Mar. Ecol. Prog. Ser. 66, 183–195.

Wassmann, P., Andreassen, I.J., Rey, F., 1999a. Seasonal variation of nutrients and suspended biomass along a transect on Nordvestbanken, north Norwegian shelf, in 1994. Sarsia 84, 199–212.

Wassmann, P., Ratkova, T., Andreassen, I., Vernet, M., Pedersen, G., Rey, F., 1999b. Spring bloom development in the marginal ice zone and the central Barents Sea. P.S.Z.N.I.: Mar. Ecol. 20, 321–346.